IEEE Access
Multidisciplinary | Rapid Review | Open Access Journal

Received November 1, 2020, accepted November 25, 2020, date of publication December 1, 2020,
date of current version December 15, 2020.

Digital Object Identifier 10.1109/ACCESS.2020.3041784

Comprehensive Analysis of Temperature and Stress Distribution in Optical Fiber Composite Low Voltage Cable Using Finite Element Method

AHSAN ASHFAQ[1], (Member, IEEE), YU CHEN[1], (Senior Member, IEEE), KAI YAO[1], (Member, IEEE), FENG JIA[1], JING YU[2], AND YONGHONG CHENG[1], (Senior Member, IEEE)

[1]State Key Laboratory of Electrical Insulation and Power Equipment, Xi'an Jiaotong University, Xi'an 710049, China
[2]Shanghai Electric Cable Research Institute, Shanghai 200093, China

Corresponding author: Yu Chen (chenyu@xjtu.edu.cn)

This work was supported by the National Key Research and Development Program of China under Grant 2016YFB0901200.

ABSTRACT Optical fiber composite low voltage cable (OPLC) is an optimized way of carrying out the function of supplying electrical power and communication signals in a single cable. In this paper, the temperature and stress distribution in OPLC cable is analyzed by using the finite element method as the current increases to maximum capacity. The increase of temperature and stress are the two main factors that affect the additional attenuation in optical fiber. This additional attenuation can be reduced by selecting the optimal heat resistant layer for the optical unit that limits the increase of temperature and stress at the optical fiber. The analysis is carried out for three different kinds of materials by using the finite element method FEM and among them, thermoplastic elastomer TPE is chosen as a heat resistant layer as it restricts the temperature and stress at rated current of 92 A to the minimum values of 69°C and 7.90×10^7 N/m^2 respectively. The OPLC cable with TPE as a heat resistant material for the optical unit is put in the experimental setup to analyze the temperature and stress increase inside the cable in real-time using the BOTDA analyzer at normal and under overload condition and compared with the simulation results to verify the correct selection of optimal heat resistant layer for optical unit.

INDEX TERMS Attenuation, current density, finite element simulation, multi-field coupling model, stress distribution, thermal field.

I. INTRODUCTION

Two-way communication between the grid and the user is the main aspect of the smart grid distribution system. This two-way communication can elegantly and optimally perform by optical fiber composite low voltage (OPLC) cable [1]. OPLC cable is a way to control the load from the electricity generating stations and means to carry out the demand side management to reduce the peak hours of the load by reducing the risk of blackouts [2]. In OPLC cable, the optical unit is stranded together with the conductors, serving both functions of transmitting power and communication in a single cable [3], [4]. The OPLC cable is used in the distribution networks having a low power rating of 1 kV. OPLC is constructed on an idea of power fiber to the home (PFTTH) [5]. This cable can integrate the electrical distribution networks with a communication network to connect the smart grid with smart meters [6]. In China, after the successful implementation of optical fiber-composite PVC insulated drop wire (OPDV) and optical fiber ground wire (OPGW) by State Grid Corporation of China, dominant support is gained by OPLC from the government to be mounted in distribution networks [7], [8]. A lot of work has been done in analyzing the electrostatic and magnetic field in submarine cables having the optical fiber serving as a sensor for monitoring the temperature distribution inside the cable [9]. Dmitriev did the electrical and thermal analysis of optical ground wire cables by using the finite element method by integrating the coupled equations [10]. Guoda did the electrothermal analysis of low and medium voltage cables using the finite

The associate editor coordinating the review of this manuscript and approving it for publication was Hui Ma.

element method [11]. Yuqing did the condition monitoring of OPLC cable by using the optical fiber temperature monitoring technology [1]. In previous researches, the work that had been carried out by most of the researchers is related to the electric field analysis, thermal analysis, magnetic field analysis, structural optimization by considering the thermal field and condition monitoring [12]–[14]. The simulation study was conducted by Wang on the optical fiber to relate the increase of stress due to increase of temperature in bare optical fiber [15] but the study was not enough because of an absence of experimental setup also the simulation study includes only the bare fiber. The study of selection of heat resistant layer for the optical unit of OPLC cable by analyzing the increase of temperature and stress is conducted for the first time in this paper along with the simulation and experiment results. Before going into the manufacturing phase it is the need of the hour to analyze the possible factors that can affect the performance of the OPLC cable, so in this paper, the temperature and stress distribution in OPLC cable is being analyzed. The structure of OPLC cable is simulated in COMSOL by using the finite element method. As the current flow in the conductors, the heat is generated due to the resistive property of conductor that causes the increase of temperature in the cable. The temperature rise due to the current flowing in the cable results in the expansion of layers due to their thermal expansion coefficient that generates the stress in the cable [16]. The internal stress generated in the OPLC cable can cause the deformation of optical fiber structure that results in attenuation [17], [18]. In the normal operating condition, the current flow in the cable caused the temperature of the conductor to increase and due to the different thermal coefficients of insulation layers, the heat is transferred towards the outer layers by creating a thermal field within the cable. The stress is generated due to the increase in temperature that forces the insulation layers to expand at different temperatures and create stress in the cable [19].

In this paper, the structure of OPLC cable and materials in the insulation of OPLC cable are explained. The thermal field distribution and thermal stress in normal operating conditions and overload conditions simulation by using the coupled equations in COMSOL for the selection of the most suitable heat resistant layer that can restrict the increase of temperature and stress to the minimum level. The selected heat resistant layer is used in the sample of the cable for the experiment. The experimental platform is set up to analyze the increase in temperature and stress in the cable by using the Brillouin optical time-domain analysis as the current flows in the conductors and the experimental results are compared with the simulated results.

II. PROBLEM DESCRIPTION

The OPLC cable is designed to use for carrying out the functions of transmitting electricity as well as the communication signal. The cable consists of different insulation layers, as the temperature at the conductor rises, the heat transfers to the outer layers causing the rise in the temperature at the optical unit that is stranded along the conductors. The increase in temperature causes the insulation layers to expand by generating stress within the cable. This increase in temperature and stress is the reason to increase the attenuation in optical fiber [18]. The block diagram of the generation of temperature and stress in a cable is shown in Fig. 1. In the block diagram two prominent factors, temperature, and stress are shown that contribute to the attenuation of communication signals.

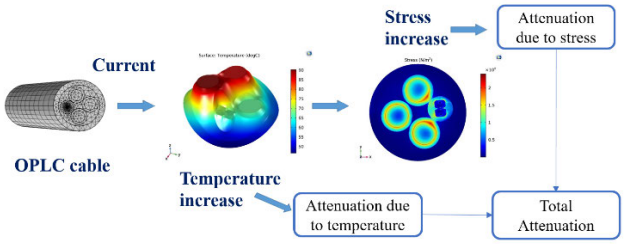

FIGURE 1. The system diagram of OPLC cable comprises temperature and stress being prominent factors in influencing the attenuation loss.

The objective of the research is to minimize the attenuation in the optical fiber signal occurs due to the increase of temperature and stress. To attain the goal, these two factors, temperature and stress have to be restricted to their minimum value. One of the problems in the OPLC project is the appropriate choice of heat resistant material that can limit the temperature and stress to the minimum value so that the attenuation in the fiber can be minimized. The other problem is to accurately analyze the increase in temperature and stress in the cable at the rated current of OPLC cable.

The first problem of choosing the material for the heat resistant layer is solved in this paper by using the coupled equations model by applying the finite element method using the COMSOL Multiphysics software. Three different types of materials are analyzed for the increase in temperature at the optical fiber as the temperature of the conductor becomes 90°C. The material that allows the minimum increase in temperature and stress at the optical fiber is chosen as the heat resistant layer. The second problem, to analyze the accurate increase in the stress and temperature in the cable is solved by putting the cable in the experiment setup. In the experiment setup, the temperature and stress inside the cable are analyzed by using the Brillouin optical time-domain analysis (BOTDA) technique. The experiment results are compared with the simulation results obtained by using the coupled equations in COMSOL Multiphysics software.

III. STRUCTURE AND MATERIALS OF OPLC

OPLC cable consists of an electrical power transmitting conductor stranded together with the optical unit. There are different structures of OPLC cables consisting of the 3-phase cable and 1-phase cable [20]. OPLC-WDZ-YJY-0.6/1kV-3x10+GQ-2B6a is a single-phase cable having phase, neutral, and earth wire along with the optical unit that comprises the optical fiber. Each conductor has an area of 10 mm^2

and the insulation of cross-linked polyethylene XLPE having a thickness of 0.7 mm. The outer insulation layer of the OPLC cable is polyethylene (PE) having a thickness of 1.8 mm. The insulation materials used in the optical unit are heat resistant layer, for heat resistant layer three materials polyethylene PE, cross-linked polyethylene XLPE, and thermoplastic elastomer TPE are taken under consideration. The modeling of the cable is shown in section 4. OPLC-WDZ-YJY-0.6/1kV-3x10+GQ-2B6a is shown in Fig. 2.

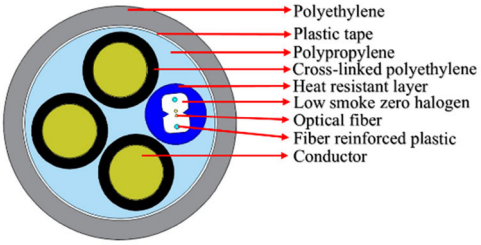

FIGURE 2. The structure and materials of OPLC cable.

The properties of materials used in the cable include thermal conductivity "k", density "ρ", thermal coefficient "α", and specific heat capacity "C_P", given in TABLE 1.

TABLE 1. Properties of materials.

Material	k [W/m·k]	ρ [kg/m^3]	α [1/K]	C_P [J/kg·K]
PE	0.480	930.0	150×10^{-6}	2100
Copper	401.0	8960	16.5×10^{-6}	384.0
PP	0.220	946.0	90.0×10^{-6}	1920
XLPE	0.290	920.0	100×10^{-6}	2930
FRP	0.550	1970	20.0×10^{-6}	1200
Fiber	1.300	730.0	0.75×10^{-6}	730.0

IV. MATHEMATICAL AND FEM MODELLING

OPLC cable is modeled in COMSOL Multiphysics to analyze the temperature and stress increase as the AC flows in the cable [21]. Previously ELEFANT 2D software was used to analyze the temperature distribution in cable [22]. In COMSOL, the study includes the heat transfer with the magnetic field to make the AC flow in the cable and calculate the temperature field distribution [23]. Solid mechanics is included in the simulation study to simulate the thermal stress developed between the layers of the cable. In a magnetic field, the AC flows through the axis of the cable. Maxwell's equations for the frequency domain are used to find the solution for magnetic fields [24]. The magnetic field density produced the current and the relationship is given by ampere's law as in (1).

$$\nabla \times H = J \tag{1}$$

Here H is the magnetic field density and J is the current density. Maxwell's Ampere law gives the relationship of electric field intensity with the current density. This relationship is further used in the study of the magnetic field in COMSOL to generate the electric field in the conductor to get the current density given in (2).

$$J = \sigma(E + v \times B) + J_e \tag{2}$$

Here σ is the electric conductivity, E is the electric field intensity, v is the velocity of conductor and B is the magnetic flux density. J_e is termed as the externally applied current density. In the simulation model, electromagnetic waves are used to generate the current. As the dielectric hysteresis and magnetic losses are neglected that leaves only the resistive losses Q_{rh} to generate the heat in the conductor due to electromagnetic losses as in (3) [26].

$$Q_{rh} = \frac{|J|^2}{2\sigma} = \frac{\mathrm{Re}(J \cdot E^*)}{2} \tag{3}$$

The first law of thermodynamics is used in the simulation to calculate the heat transfer in solids that include resistive losses due to electromagnetic waves. The equation for current density is coupled with the production of heat due to resistive losses. The heat equation is expressed in temperature T instead of internal energy U as in (4).

$$\sigma C_P \left(\frac{\partial T}{\partial t} + (u \cdot \nabla)T\right) = -(\nabla \cdot q) + \tau : \varepsilon - \frac{T}{\rho}\frac{\partial \rho}{\partial T}\bigg|_p \left(\frac{\partial p}{\partial t} + (u \cdot \nabla)p\right) + Q \tag{4}$$

Here C_p is the specific heat capacity J/kg · K, T is the temperature in kelvin K, ρ is the density kg/m^3, u is the velocity vector m/s, q is the heat flux by conduction W/m^2, τ is the viscous stress tensor Pa, p is the pressure N/m^2, ε is the strain-rate tensor 1/s, used as the structural mechanics is included in the simulation to calculate the stress in the cable. As the mass is always been conserved so the density and velocity are related as in (5).

$$\frac{\partial \rho}{\partial t} + \nabla \cdot (\rho v) = 0 \tag{5}$$

Fourier's law of heat conduction states the conductive heat flux is proportional to the gradient of temperature as in (6) [25], [26].

$$q = -k\frac{\partial T}{\partial x} \tag{6}$$

Here k is the thermal conductivity (W/m · K). Inserting the above equations in the heat equation, the equation gets simplified as (7).

$$\rho C_P \frac{\partial T}{\partial t} + \rho C_P u \cdot \nabla T = \nabla \cdot (k\nabla T) + Q \tag{7}$$

Here the heat due to electromagnetic resistive losses Q_{rh} is given as in (8).

$$Q_{rh} = -\nabla \cdot (k\nabla T) \tag{8}$$

The temperature rise caused the deformation of the structure of the cable due to the thermal expansion coefficient of

different insulation materials. The expansion caused stress between the insulating layers. This stress is calculated by including the study of solid mechanics. The interface of solid mechanics defines the deformation of solid objects in the physical space called a spatial frame. When the solid object distorts due to internal thermal stress, every particle keeps its reference coordinates X, while the spatial coordinates 'x' of the material change with time as (9).

$$x = X + u(X, t) \tag{9}$$

Here u is the displacement vector that points from the reference to the current position, determined the spatial position. The gradient of the displacement is computed in terms of material coordinates as (10).

$$\nabla u = \begin{bmatrix} \frac{\partial u}{\partial X} & \frac{\partial u}{\partial Y} & \frac{\partial u}{\partial Z} \\ \frac{\partial v}{\partial X} & \frac{\partial v}{\partial Y} & \frac{\partial v}{\partial Z} \\ \frac{\partial w}{\partial X} & \frac{\partial w}{\partial Y} & \frac{\partial w}{\partial Z} \end{bmatrix} \tag{10}$$

Here, u, v, and w are the global Cartesian components of displacement vector in the spatial frame, and X, Y, and Z are the material coordinate variables. The strain tensor ε is calculated by using the displacement gradient as (11).

$$\varepsilon = \frac{1}{2}(\nabla u^T + \nabla u) \tag{11}$$

The system model used in COMSOL, integrating the heat transfer with the structural mechanics model is shown in Fig. 3. The system model shows the interconnection of equations and their influence.

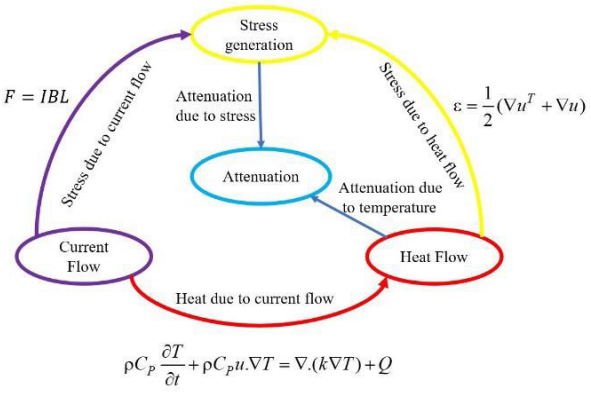

FIGURE 3. Coupled equations for applying FEM in COMSOL.

The model is built in AutoCAD software and geometry is exported in COMSOL. The material properties of the cable are added. The study of a magnetic field is integrated with the study of heat transfer in solids to get the temperature increase in the cable. The boundary condition of the simulation is the outside environment temperature that is taken at 20°C. The mesh is applied to the cable structure and is shown in Fig. 4.

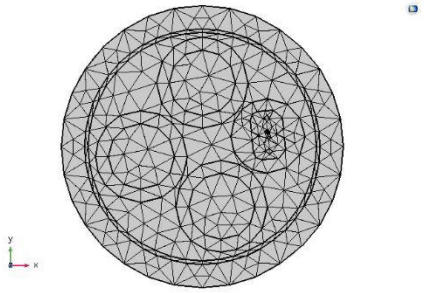

FIGURE 4. The meshing of OPLC cable for applying FEM in COMSOL.

A. ANALYSIS OF TEMPERATURE FIELD DISTRIBUTION USING FEM

The first material is chosen to be polyethylene PE. PE has been one of the top choices in the insulation materials for cables having a thermal conductivity of 0.480 W/m · K. The temperature of the conductor begins to increase as the AC flows in the conductor causing the heat to flow towards the outer insulation layer. At the maximum temperature of 90°C for normal operating conditions for cross-linked polyethylene XLPE insulated conductors, the temperature of the optical unit is increased to 72°C. The overload current is termed as the current that makes the temperature of the conductor rise to 10% of its maximum limit of 90°C that is 99°C. At 99°C, the temperature of the optical fiber becomes 78.06°C.

The second material is chosen to be cross-linked polyethylene XLPE. It is the popular insulation material for the cables having a low thermal conductivity of 0.285 W/m·K. The low thermal conductivity allows it to restrict the temperature increase across the insulation layer. As the temperature of the conductor becomes 90 °C due to the heat transfer, the temperature of the optical unit is increased up to 71.27°C. Under an overload condition, the temperature of the optical fiber becomes 77.81°C.

The third material is thermoplastic elastomer TPE having a low thermal conductivity of 0.180 W/m · K, makes it one of the competent candidates for the heat resistant layer. The flow of AC causes the temperature of the conductor to rise to 90 °C and as the heat is transferred the temperature of the optical unit increased to 70°C that is shown in Fig. 5. Thermoplastic elastomer restricts the increase in temperature at optical fiber better than the PE and XLPE. At an overload condition that is 99°C, the temperature of the optical fiber becomes 76.5°C.

The optical unit is placed away from the center of the cable to minimize the increase of temperature as the temperature in the center of the cable is relatively higher than the side of one conductor because in the center heat is transmitted from both conductors. The temperature is further decreased to 2°C at the optical fiber as TPE is used as a heat resistant layer for optical unit. The temperature distribution in the OPLC cable by using PE, XLPE, and TPE at different parts of the cable are shown in Table 2.

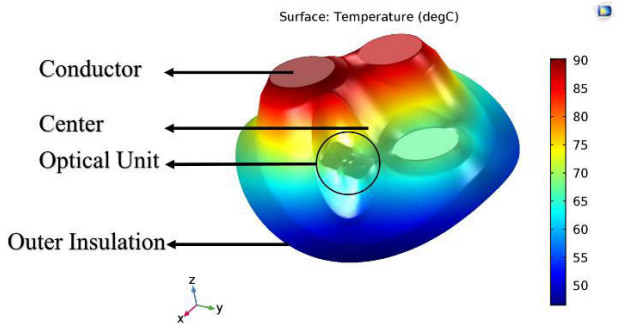

FIGURE 5. Temperature field distribution by using TPE as a heat resistant layer.

TABLE 2. Temperature distribution in OPLC cable.

Material	Conductor [°C]	Center of cable [°C]	Optical Unit [°C]	Outer insulation [°C]
PE	90	83.0	72.00	55
XLPE	90	82.6	71.27	53
TPE	90	81.5	70.00	49

It is evident from the above simulations that TPE restricts the increase of temperature at the optical fiber comparatively better than PE and XLPE. The temperature increase can be restricted more by using the optimization algorithms that include the constraints of increasing or decreasing the layer width but at the current stage of the project, the study is conducted on the selection of heat resistant layer that can limit the increase of temperature and stress. We have fixed the width of the heat resistant layer and placed the optical fiber away from the conductors because the temperature at the conductors is at its highest value that can cause more temperature increase if the optical unit is placed in the center of the cable near to the conductors. If the width of the heat resistant layer is increased, the temperature might decrease a little but this will cause an increase of stress as there will be more expansion of insulation layers due to the thermal expansion coefficient of material and increase of stress at the fiber will contribute in attenuating the signal in optical fiber.

B. ANALYSIS OF STRESS FIELD DISTRIBUTION USING FEM

The temperature distribution in three materials PE, XLPE, and TPE show the minimum temperature increase in TPE that makes it the best option for the heat resistant layer. TPE has the lowest thermal conductivity of 0.180 W/m · K that restricts the temperature increase inside the optical unit and has the highest poisons ratio of 0.48 and Young's modulus of 2.9×10^9 N/m^2 that makes it incompressible. The TPE compresses relatively less than the other two materials and exerts less external pressure inside the optical unit. The temperature rise causes stress to be generated in the cable. In the conducted study the stresses due to the manufacturing process along with the stress due to the magnetic field generated by flow of current in conductors are not considered. The stress due to magnetic field is neglected because of the presence of polypropylene that restricts the stress due to magnetic field to move towards the optical unit of optical fiber. This leaves us with thermal stress. This thermal stress is calculated by adding the study of structural mechanics in the simulation. In structural mechanics, the strain tensor is calculated as the materials expand due to the thermal expansion coefficient. The strain tensor and initial stress are used to calculate the stress in the cable by using the finite element method. This thermal stress forces the optical fiber layers to be deformed [27]. The stress is simulated in above mentioned three materials. At the maximum point of normal operating condition, PE having poisons ratio of 0.46 and Young's modulus of 8×10^8 N/m^2, produced the stress of 8.48×10^7 N/m^2, XLPE having poisons ratio of 0.42 and Young's modulus of 7×10^8 N/m^2, produced the stress of 8.22×10^7 N/m^2 and TPE, having the highest poisons ratio of 0.48, produced the stress of 8.07×10^7 N/m^2. This makes the TPE is our best choice for heat resistant layer that can not only restricts the temperature increase but also produced the minimum stress at the optical fiber. The stress produced by three materials in normal and overload conditions is given in Fig. 6.

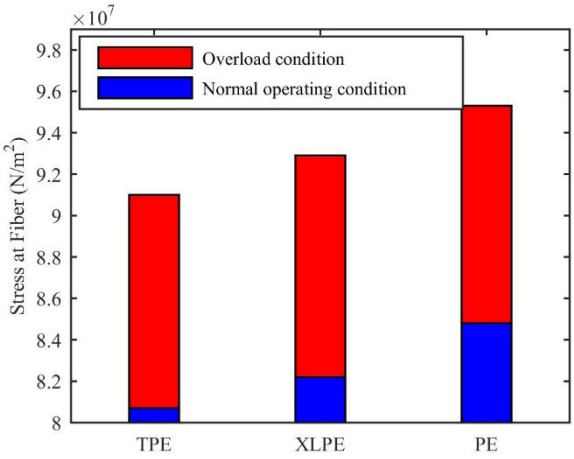

FIGURE 6. Stress is generated at optical fiber by TPE, XLPE, and PE as a heat resistant layer.

The temperature and stress on the optical fiber rise to 70 °C and 8.07×10^7 N/m^2 respectively as the current of 92 A flows in the conductor of OPLC cable. The increase in temperature results in the thermal expansion of insulation layers that causes stress. These two prominent factors contribute to deforming the structure of optical fiber resulting in the attenuation in the optical signal. The attenuation becomes worse in the short circuit faults [28]. After computing the simulation for analyzing the stress, we can see the stress distribution in a cable as shown in Fig. 7.

In COMSOL, structural mechanics is added that links the heat transfer module with the solid mechanics. In this way, simulation is carried out that calculates the amount of stress

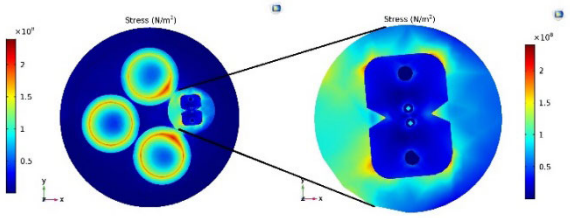

FIGURE 7. Stress distribution in OPLC cable by using TPE as a heat resistant layer.

generated in the cable as the heat flow in the conductors. The dark blue areas that are away from the conductors show the low stress and the light areas show the high-stress concentration at the optical fiber in the cable. One side that is close to the conductors shows more stress due to the expansion of layers in the cable.

The above simulation results make the TPE the most suitable choice for the heat resistant layer for the optical unit of OPLC cable. The TPE is used as the heat resistant layer in the manufacturing of OPLC cable and the cable is put in the experiment platform to analyze the increase of temperature and stress in real-time at normal operating conditions and under overload conditions. The experimental analysis for the increase of temperature and stress at different current levels are given in section V.

V. EXPERIMENTAL ANALYSIS

The optical unit in the cable is used to measure the strain inside the cable. The increase in strain is analyzed by using Brillouin optical time-domain analysis (BOTDA). BOTDA technology is a measurement technique that indicates the increase of temperature and strain along with the optical fiber. In the BOTDA sensing technique, the pump and probe light is injected from the starting and ending points of optical fiber respectively. The disturbance due to temperature and strain makes the frequency difference between pump and probe light, this difference equals the frequency shift. The frequency shift ν_B *has* a linear relationship with the change of strain and the change of temperature in the optical fiber. This linear relationship is being used by BOTDA to calculate the change of temperature and strain along with the fiber. The change in strain, temperature and Brillouin frequency shift of the fiber can be expressed as (12).

$$\nu_B = C_\varepsilon \Delta_\varepsilon + C_T \Delta T + \nu_{B0} \tag{12}$$

Here, ν_B is the frequency shift as ε is the axial strain, ν_{B0} is the reference frequency shift without the change in strain, C_ε is the coefficient of strain, C_T is the coefficient of temperature, $\Delta\varepsilon$, and ΔT is the change in strain and temperature, respectively. The strain ε is put in (13) to get the stress σ at the optical fiber. Here E is the young's modulus of optical fiber.

$$\sigma = E \cdot \varepsilon \tag{13}$$

In Section IV, simulation is done by using three different materials for the heat resistant layer. Thermoplastic elastomer TPE turns out to be the best among them. Based on the simulation results TPE is used in the manufacturing of the real cable sample and the sample of OPLC cable is put in the experiment setup to analyze the increase of temperature and strain in real-time as the current flows in the cable. To accurately measure the increase of strain in cable, a BOTDA analyzer is used. BOTDA analyzer records the frequency shift that increases due to the increase of temperature and strain. The frequency shift along with the increase of temperature measured by temperature sensors inserted in the cable is put in (12). Two experiments are conducted in Section V to analyze the coefficient of temperature C_T and coefficient of strain C_ε. These coefficients vary slightly for different kinds of optical fiber. To measure the accurate value of strain in OPLC cable the value of temperature coefficient C_T and strain coefficient C_ε are put in (12) along with the increase of frequency shift recorded in the experiment of analyzing temperature and strain in OPLC cable by using BOTDA.

A. ANALYSIS OF TEMPERATURE AND STRAIN COEFFICIENT

The temperature influence coefficient C_T is different for each fiber. The linear relationship is developed between the frequency shift and the change of temperature by analyzing the frequency shift as the temperature of the optical fiber is changed. The optical fiber of 100m length is put in the temperature controller. The two ends of optical fiber are connected to the BOTDA analyzer. The pump and probe light is injected to both ends respectively. The temperature of the controller is set to 20 °C and the optical fiber is put in the controller. The temperature of the controller is then increased with the step size of 10 °C and the Brillouin fiber time-domain analysis was repeatedly carried out up to 70 °C. The frequency shift obtained at different temperature levels is then put in (12) to get the temperature coefficient C_T. The experiment setup is shown in Fig. 8.

The Brillouin frequency shift increases as the strain in the fiber increase making the linear relationship between the frequency shift and the applied strain. To get this linear relation, the strain is produced in the single-mode fiber and frequency shift is recorded at the same time by using BOTDA. To produce the strain in optical fiber, one end of the fiber is attached to the fixed end and the other end is attached to the movable end. Both ends of the optical fiber are connected to the BOTDA. The optical fiber is attached in a strain-free state. The reference frequency shift is recorded in a strain-free state of optical fiber. The controlled displacement is given to the high-precision displacement platform of 0.01 mm and at the same time the BOTDA recorded the frequency shift. The BOTDA analyzer recorded the data up to 0.05 mm displacement given by high-precision displacement platform to produce the strain in the optical fiber. The frequency shift and increase in strain is put in (12) to get the value of coefficient of strain as 0.052 MHz/$\mu\varepsilon$. The experimental platform is shown in Fig. 9.

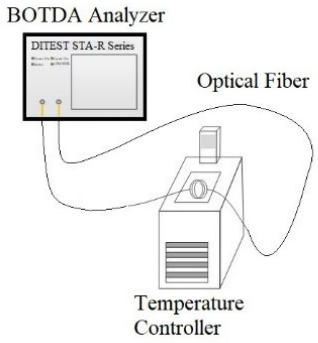

FIGURE 8. Experimental platform for calibration of temperature coefficient.

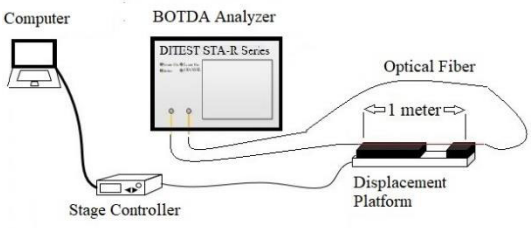

FIGURE 9. Experimental platform for calibration of strain coefficient.

B. ANALYSIS OF TEMPERATURE AND STRAIN IN OPLC CABLE

In the experimental setup, the temperature and stress in the OPLC cable are analyzed by injecting the current to flow in conductors. The flow of current resulted in the increase of temperature that is being measured by temperature sensors inserted in the OPLC cable and an increase of thermal stress is measured by calculating the strain by BOTDA analyzer. The OPLC cable used in the experimental setup has TPE as a heat resistant layer. In OPLC cable there are two single-mode fibers (SMF), SMF-1 is connected to the BOTDA analyzer and SMF-2 is connected to the light source and power energy meter to ensure the continuity of optical signal during the current flow. Optical fiber splicer is used to connect the optical fiber with the connector having a loss of 0.01 dB, the two ends of the SMF-2 is connected with the Thorlabs S155C connector having the capacity to transmit 20 mW of power from the light source to the power energy meter. One end of SMF-1 is connected to the probe end of BOTDA and the other end is connected to the pump end of BOTDA. The current is produced in the cable by the magnetic field generated by the high current generator that is controlled by the variable transformer. The OPLC cable passed through the core of the current generating transformer that generates the magnetic field resulting in the generation of current in the cable. The variable transformer is used to control the current generated in the OPLC cable. The variable transformer is connected with the primary winding of the current generator that controls the value of current. The cable is cut open and temperature sensors are placed inside at different points of cable and after placing the temperature sensors the cable is put into the original closed state. The temperature sensors are placed at different points inside the cable to measure the temperature of the conductors and optical fiber as the current flows inside the cable. The data acquisition module is used for the computer interface to save the temperature data in real-time. The variable transformer is used to regulate the current at different levels and kept the same level of current for 2 hours until the temperature inside the cable became constant. As the temperature becomes stable inside the cable BOTDA records the frequency shift. The experiment platform is shown in Fig. 10.

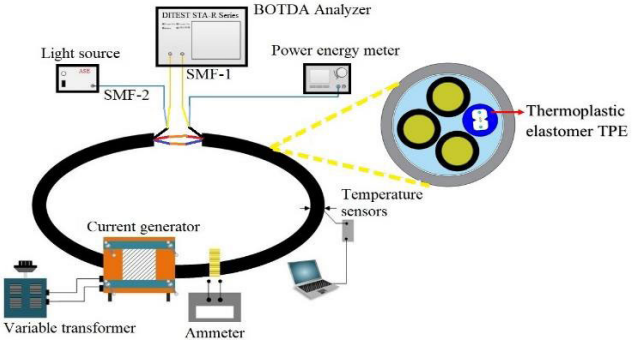

FIGURE 10. Experimental platform for analyzing the increase in temperature and strain in OPLC cable.

VI. RESULTS AND DISCUSSION

A. RESULTS

1) ANALYSIS OF TEMPERATURE COEFFICIENT

For single-mode fiber, the BOTDA analyzer recorded the frequency shift at temperature starting from 20°C to 70°C with a step size of 10°C. The recorded frequency shift with temperatures is fitted in MATLAB curve fitting that gave the value of temperature coefficient of 1.089 MHz/°C. The obtained value of the temperature coefficient is in a good range with the Brillouin temperature coefficient delivered by most manufacturers. The results of the frequency shift are recorded by BOTDA analysis and put in (12) to get the temperature coefficient C_T. The results indicate the linear relationship of frequency shift with the increase in temperature. The results are shown in Table 3, with MATLAB fitting curve in Fig. 11.

TABLE 3. Frequency shift for temperature levels at the optical fiber.

The temperature at optical fiber [°C]	Frequency Shift [GHz]	Temperature coefficient [MHz/°C]
20	10.836	1.100
30	10.846	1.060
40	10.855	1.105
50	10.865	1.116
60	10.876	1.113
70	10.886	1.097

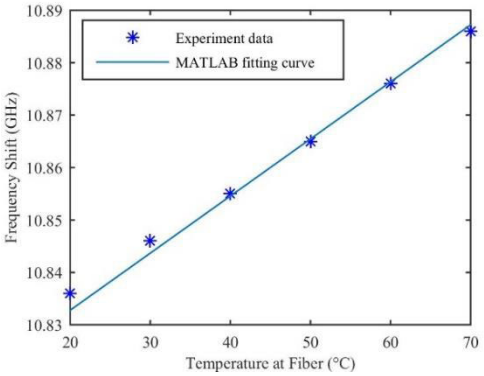

FIGURE 11. MATLAB fitting curve to get temperature coefficient.

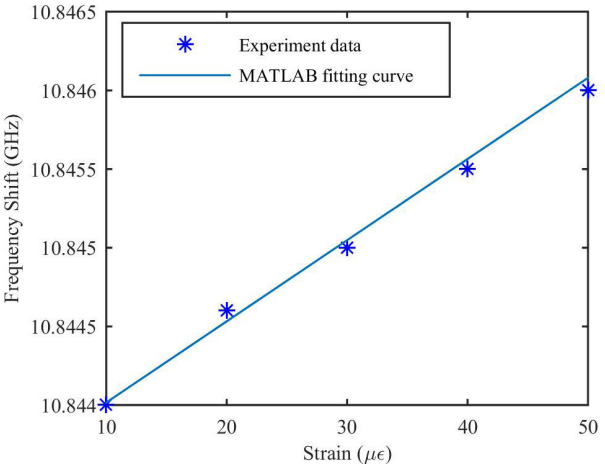

FIGURE 12. MATLAB fitting curve to get strain coefficient.

2) ANALYSIS OF STRAIN COEFFICIENT

The frequency shift recorded by using Brillouin optical time-domain analysis is given in Table 4. The coefficient of strain is calculated by (12) as 0.052 MHz/$\mu\varepsilon$ by the MATLAB fitting curve. The calculation is done by taking the change of temperature as 0°C as there is no temperature change as the strain is generated in the single-mode optical fiber. The value of temperature and strain coefficients are used in (12) to get an increase in temperature and strain in OPLC cable as the current flow in the conductors is normal and under overload conditions.

TABLE 4. Frequency shift for strain levels at the optical fiber.

Displacement [mm]	Frequency Shift [GHz]	Strain coefficient [MHz/με]
0.01	10.8440	0.051
0.02	10.8446	0.053
0.03	10.8450	0.052
0.04	10.8455	0.051
0.05	10.8460	0.051

The MATLAB fitting curve between the frequency shift and strain $\mu\varepsilon$ is shown in Fig. 12.

3) ANALYSIS OF TEMPERATURE AND STRAIN IN OPLC CABLE

The experiment started with no current in the cable and the BOTDA analyzer recorded the initial frequency shift having initial temperature and initial strain that is used as the reference value. The current of 20 A is injected in the cable for 2 hours to stabilize the temperature increase within the cable. As the temperature in the cable becomes stable the BOTDA analyzer again measures the frequency shift for the temperature and strain measurement. The process is repeated with the step size of 20 A current until the temperature of the conductor reached up to the overload condition of 99°C. The increase of temperature in the conductor and optical fiber with the increase of current is measured by using the temperature sensors inserted inside the cable. The BOTDA analyzer recorded the frequency shift at the current levels with a step size of 20°C. The temperature of conductor and optical fiber simulated in COMSOL is compared with the experimental results and shown in Fig. 13.

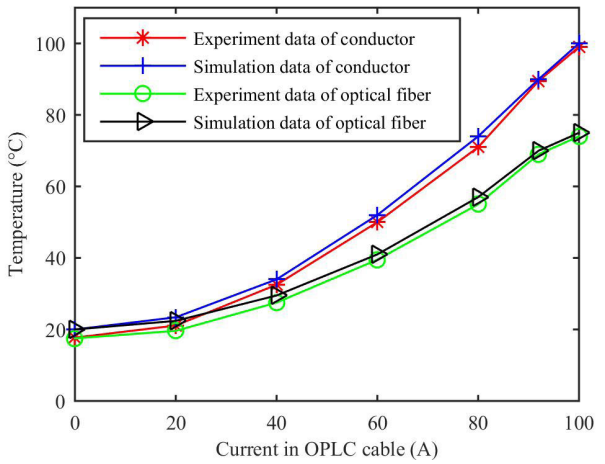

FIGURE 13. The temperature increase in the conductor and optical fiber as the current flow in OPLC cable.

The maximum operating temperature for XLPE insulated conductors is taken at 90°C which occurs at 92 A of current. The length of the cable is 10 meters starting from 5 m to 15 m. The first 5 meters of fiber include the connecting fibers from cable to the BOTDA analyzer. The frequency shift at different current levels is shown in Fig. 14.

The starting end of the cable is connected with the optical fiber that is further connected to the BOTDA analyzer. The frequency shift at 92 A current is also recorded by the BOTDA analyzer. As the current increased, the temperature and stress at the optical fiber increased and the increasing Brillouin frequency shift is the proof. The Brillouin frequency shift for 0 A current is taken as reference and (12) is used to find the strain in the optical fiber. The Brillouin frequency shift, temperature coefficient, temperature of optical fiber,

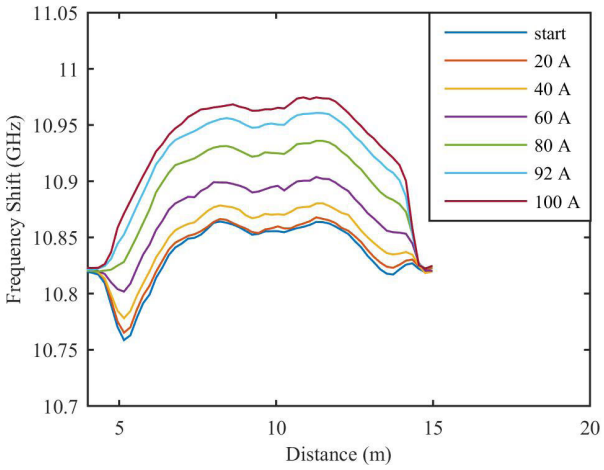

FIGURE 14. Brillouin frequency shifts due to stress and temperature in the OPLC during the operating condition.

and strain coefficient is put in (12) to get the strain. This strain is then put in (13) to get the stress in optical fiber. The increase in stress in the experimental analysis compared with the simulated stress is shown in Fig. 15.

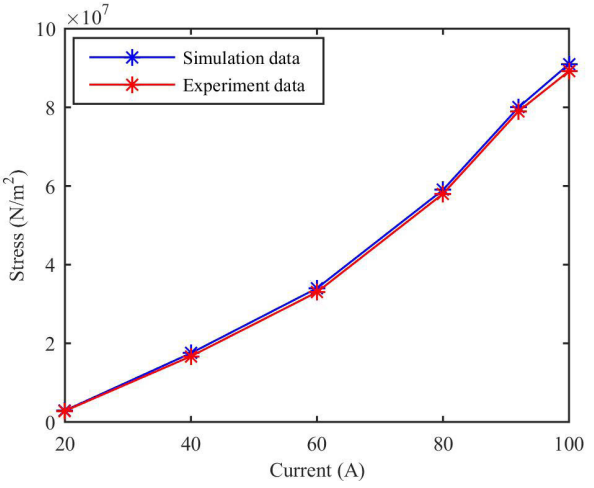

FIGURE 15. Stress increase with the increase of current.

B. DISCUSSION

In OPLC cable the optical unit is stranded with the conductors and the flow of current in the conductors generates the increase in temperature and stress on the optical fiber that is capable of influencing the attenuation in the optical signal. The increase in attenuation of the signal has a direct relation with the increase of temperature and stress so currently, the research carried out in this paper is more focused on the selection of heat resistant layer for the optical unit of OPLC that restricts the temperature and stress to the value as minimum as possible. At the current stage of the project, the experiment is performed on OPLC cable of 10-meter length. To relate the attenuation with temperature and strain, 1 km long OPLC cable is required because it is the only way to correctly analyze and relate the attenuation with temperature and stress. The state of the art power source and power energy meter has a fluctuation error of $\pm$0.003 dB/km. The standard for optical fiber communication is 0.15 dB/km, which means that for 10-meter cable the attenuation must be below 0.0015 dB/km that is not possible to measure with the currently available equipment. For that 1 km long OPLC cable is required, so at the current stage of project it is not possible to relate the attenuation with the increase of temperature and stress experimentally. As the attenuation of signal has a direct relation with temperature and stress so by decreasing the increase of these two factors it is possible to decrease the attenuation in signal. To decrease the effect of these factors, an appropriate heat resistance layer is chosen as the outer insulation material for the optical unit. For the heat resistance material, a thermoplastic elastomer is selected as it restricts the temperature and stress to its minimum limit.

In the simulation section thermoplastic elastomer TPE shows relatively better performance than polyethylene PE and cross-linked polyethylene XLPE in restricting the increase in temperature and strain due to its low thermal conductivity and high poisons ratio. The low thermal conductivity restricted the increase of temperature and the high poisons ratio restricted the materials to expand upon the temperature increase that further helped to decrease the stress generated due to thermal expansion of heat resistant layer on the optical fiber. Due to these promising features TPE is used as the heat resistant layer in OPLC cable sample to be put in the experiment setup. In the experiment set up as the temperature sensors are inserted inside the cable so in the process, there is a small chance of leakage of heat from the cable that is the reason, the simulation temperature is slightly higher than the experiment results. The increase of temperature and stress due to the current flow is inevitable but the optimal choice of heat resistant layer helped to restricts the increase of temperature and stress to the minimum value. As the current begins to flow the temperature at the conductors begins to rise due to the resistive losses of the conductor. This temperature increase causes the insulation layers of the OPLC cable particularly the heat resistant layer of optical unit to expand in all directions. The expansion of heat resistant layer towards the optical fiber generates stress on the optical fiber. The increase in temperature attenuates the communication signal and the stress generated due to the increase of temperature further attenuates the signal. To reduce the attenuation in optical fiber it is necessary to restrict these two factors to their minimum value possible.

In normal operating conditions, the maximum current of 92 A in the OPLC cable makes the temperature of the conductor rise to 89.7°C. The temperature is distributed in the cable and the experiment results illustrated that the temperature at the optical fiber rise to 69°C. The increase in temperature in the OPLC cable caused the insulation layers to expand which resulted in the stress between the layers of the OPLC cable. The Brillouin optical time-domain analysis

is performed while the current circulated in the OPLC cable. SMF-1 is connected to the BOTDA analyzer to measure the frequency shift as the temperature and stress began to rise with the rise of current. This frequency shift is then used to calculate the thermal stress in the OPLC cable. The thermal stress on the optical fiber is experimentally calculated as 7.90×10^7 N/m^2 at a maximum limit of normal operating conditions of 92A. At the overload current, the experiment results illustrated that the temperature of the optical fiber became 74°C. At the overload condition, the thermal stress is experimentally analyzed as 8.92×10^7 N/m^2. It is concluded from the results that as the current increases in the cable, the temperature also rises between the layers of OPLC cable. The increase in temperature causes the layers to expand in every direction that creates stress within the insulation layers. This internal pressure caused the insulation materials to expand towards the optical fiber that generates the stress in the optical fiber. The simulation and experiment results are shown in Table 5.

TABLE 5. Comparison of simulation and experiment results.

Current [A]	Temperature at fiber [°C]		Stress at fiber×10^7 [N/m^2]	
	Simulation	Experiment	Simulation	Experiment
20	22.4	19.6	0.29	0.28
40	29.5	27.5	1.75	1.67
60	41.0	39.5	3.40	3.30
80	57.0	55.0	5.90	5.80
92	70.0	69.0	8.07	7.90
100	75.0	74.0	9.10	8.92

VII. CONCLUSION

In this paper, three materials have been simulated for analyzing the distribution of temperature and stress in OPLC cable at the optical fiber. TPE is selected as the best option as a heat resistant layer as it restricts the temperature and stress to its minimum value among PE and XLPE. It is important to restrict these two factors as these two factors are capable of affecting the performance of OPLC cable by attenuating the optical signal. As the current flows the heat generated from the conductors flows outside that causes the increase of temperature at the optical fiber. The temperature increase causes the generation of stress within the layers and this stress is capable of deforming the structure of the optical fiber. Two cases had been discussed as normal operating conditions and overload conditions. At normal operating conditions, the TPE heat resistant layer restricts the temperature and stress to 69°C and 7.90×10^7 N/m^2 respectively. Under overload conditions the temperature at the optical fiber is increased to 74°C and stress increased to 8.92×10^7 N/m^2. The increase of temperature and stress is inevitable in OPLC cable but restricting these factors to the minimum point is possible by selecting the appropriate heat resistant layer to minimize the attenuation in the communication signal.

REFERENCES

[1] L. Yuqing, Q. Liyan, L. Weiqing, G. Kunya, and T. Jie, "Study for the condition monitoring and status assessment of optical fiber composite low-voltage cable," in *Proc. IEEE Int. Conf. Electron. Commun. Eng. (ICECE)*, Xi'an, China, Dec. 2018, pp. 125–129.

[2] A. Ashfaq, S. Yingyun, and A. Z. Khan, "Optimization of economic dispatch problem integrated with stochastic demand side response," in *Proc. IEEE Int. Conf. Intell. Energy Power Syst. (IEPS)*, Kyiv, Ukraine, Jun. 2014, pp. 116–121.

[3] Y. Lei and B. Hou, "Research on fiber optical sensing technology of monitoring OPLC operation safety condition," in *Proc. 3rd IEEE Int. Conf. Comput. Commun. (ICCC)*, Chengdu, China, Dec. 2017, pp. 2722–2726.

[4] T. Vijayapriya and D. P. Kothari, "Smart grid: An overview," *Smart Grid Renew. Energy*, vol. 2, no. 4, pp. 305–311, 2011.

[5] L. Jianming, W. Jiye, F. Pengzhan, and Z. Zichao, "Application of PFTTH in smart grid," in *Proc. 13th Int. Conf. Adv. Commun. Technol. (ICACT)*, Seoul, South Korea, Feb. 2011, pp. 389–392.

[6] M. Li, W. Gu, W. Chen, Y. He, Y. Wu, and Y. Zhang, "Smart home: Architecture, technologies and systems," *Procedia Comput. Sci.*, vol. 131, pp. 393–400, Jan. 2018.

[7] A. M. Aguiar and M. S. Perez, "Experience in OPGW cables selection for overhead transmission live lines," in *Proc. IEEE/PES Transmiss. Distrib. Conf. Expo., Latin Amer.*, Caracas, Venezuela, Aug. 2006, pp. 1–6.

[8] R. V. Carvalho, M. J. D. C. Bonfim, D. A. Ussuna, L. F. R. B. Toledo, R. Martins, and V. S. Filho, "Distributed temperature sensing in OPGW with multiple optical fibres," *IET Sci., Meas. Technol.*, vol. 13, no. 8, pp. 1219–1223, Oct. 2019.

[9] I. A. Metwally, "Electrostatic and magnetic field analyses of 66-kV cross-linked polyethylene submarine power cable equipped with optical fiber sensors," *Electr. Power Compon. Syst.*, vol. 38, no. 4, pp. 465–476, Feb. 2010.

[10] L. Gonzalez and V. Dmitriev, "Electrothermal analysis of modified OPGW cables using multiphysics model," in *Proc. SBMO/IEEE MTT-S Int. Microw. Optoelectron. Conf. (IMOC)*, Porto de Galinhas, Brazil, Nov. 2015, pp. 1–5.

[11] E. Gouda and A. Z. El Dein, "Electrothermal analysis of low- and medium-voltage cable joints," *Electr. Power Compon. Syst.*, vol. 44, no. 1, pp. 101–121, Jan. 2016.

[12] X. Dong, N. Zhang, C. Kang, and H. Sun, "Analysis of power transfer limit considering thermal balance of overhead conductor," *IET Gener., Transmiss. Distrib.*, vol. 9, no. 14, pp. 2007–2013, Nov. 2015.

[13] F. Kaidanov, R. Munteanu, and G. Sheinfain, "Damages and destruction of fiber optic cables on 161 kV overhead transmission lines," *IEEE Elect. Insul. Mag.*, vol. 16, no. 4, pp. 16–23, Jul. 2000.

[14] Y. Serizawa, M. Myoujin, S. Miyazaki, and K. Kitamura, "Transmission delay variations in OPGW and overhead fiber-optic cable links," *IEEE Trans. Power Del.*, vol. 12, no. 4, pp. 1415–1421, Oct. 1997.

[15] W. Wang, Y. Liu, P. Yu, Y. Chen, J. Yu, and J. Li, "Simulation study of OPLC optical loss with effect of thermal-strain," in *Proc. 24th Opto-electron. Commun. Conf. (OECC), Int. Conf. Photon. Switching Comput. (PSC)*, Fukuoka, Japan, Jul. 2019, pp. 1–3.

[16] F. E. Seraji, "Effects of hydrostatic pressure and thermal loading on optical fibers coated with multilayer segmented Young's modulus materials," *Int. J. Opt. Appl.*, vol. 2, no. 2, pp. 6–14, Aug. 2012.

[17] D. Marcuse, "Influence of curvature on the losses of doubly clad fibers," *Appl. Opt.*, vol. 21, no. 23, pp. 4208–4213, Dec. 1982.

[18] K. Yao, Y. Chen, A. Ashfaq, G. Sun, and Y. Guo, "Power loss due to temperature rise in the optical unit of optical fiber composite low voltage cable," in *Proc. 12th Int. Conf. Properties Appl. Dielectr. Mater. (ICPADM)*, Xi'an, China, May 2018, pp. 508–511.

[19] J. D. LeGrange, H. C. Ling, and D. M. Velez, "Effects of mechanical stress on the transmission properties of optical fiber packaged in a composite structure," *Appl. Opt.*, vol. 33, no. 18, pp. 3890–3895, Jun. 1994.

[20] M. A. Shah, Y. Chen, A. Ashfaq, G. Sun, Y. Kai, L. Fu, and J. Yu, "Temperature field distribution of optical fiber composite low-voltage cable," in *Proc. Int. Symp. Electr. Insulating Mater. (ISEIM)*, Toyohashi, Japan, Sep. 2017, pp. 295–298.

[21] *Simulate Static and Low-Frequency Electromagnetics With the AC/DC Module*. Accessed: Feb. 26, 2018. [Online]. Available: https://br.comsol.com/acdc-module

[22] M. Zunec, I. Ticar, and F. Jakl, "Determination of current and temperature distribution in overhead conductors by using electromagnetic-field analysis tools," *IEEE Trans. Power Del.*, vol. 21, no. 3, pp. 1524–1529, Jul. 2006.
[23] M. Zunec, F. Jakl, and I. Ticar, "Skin effect impact on current density distribution in OPGW cables," *Elektrotehniski Vestnik*, vol. 70, no. 1, pp. 17–21, Jan. 2003.
[24] V. Dmitriev and L. Gonzalez, "Electrical and thermal analysis on optical ground wire cables in short-circuit regime by coupled equations," *Electr. Power Syst. Res.*, vol. 101, pp. 80–87, Aug. 2013.
[25] *Cable Tutorial Series*. Accessed: Apr. 26, 2017. [Online]. Available: https://www.comsol.com/model/cable-tutorial-series-43431
[26] L. Zhang, Y. He, Y. Liu, F. Yang, T. He, L. Liu, S. Wang, and H. Liu, "Temperature analysis based on multi-coupling field and ampacity optimization calculation of shore power cable considering tide effect," *IEEE Access*, vol. 8, pp. 119785–119794, 2020.
[27] W.-J. Chang, H.-L. Lee, and Y.-C. Yang, "Hydrostatic pressure and thermal loading induced optical effects in double-coated optical fibers," *J. Appl. Phys.*, vol. 88, no. 2, pp. 616–620, Jul. 2000.
[28] F. Seraji and G. Toutian, "Effect of temperature rise and hydrostatic pressure on microbending loss and refractive index change in double-coated optical fiber," *Prog. Quantum Electron.*, vol. 30, no. 6, pp. 317–331, 2006.

AHSAN ASHFAQ (Member, IEEE) was born in Punjab, Pakistan, in 1987. He received the B.E. degree in electrical engineering from the National University of Sciences and Technology (NUST), Pakistan, and the M.Sc. degree in electric power systems from the North China Electric Power University, Beijing, China, in 2014. He is currently pursuing the Ph.D. degree in electric engineering with Xi'an Jiaotong University, Xi'an, China. From 2014 to 2016, he worked as a Lecturer with the National University of Sciences and Technology (NUST). His current research interests include diagnosis on power equipment, smart grid distribution networks, and optical fiber communication.

YU CHEN (Senior Member, IEEE) was born in Hebei, China, in 1977. He received the B.S., M.S., and Ph.D. degrees in electrical engineering from Xi'an Jiaotong University, China, in 2000, 2003, and 2008, respectively. From 2008 to 2009, he was a Visiting Lecturer with the Graduate School of Information, Production and System, Waseda University, Japan. From 2009 to 2010, he was a Research Fellow with the Department of Electrical Engineering and Electronics, KIT, Japan, where he was also a Research Fellow with the Laboratory of Spacecraft Engineering Interaction Engineering, from 2010 to 2012. Since 2012, he has been an Associate Professor with Xi'an Jiaotong University, China. His research interests include on-line monitoring and diagnosis on power equipment, nanocomposite, and spacecraft charging.

KAI YAO (Member, IEEE) was born in Shanxi, China, in 1992. He received the bachelor's degree in electrical engineering from Beijing Jiaotong University, in 2015, where he is currently pursuing the degree in electrical engineering. His research interests include on-line monitoring and fault diagnosis of power equipment.

FENG JIA was born in Shanxi, China, in 1992. He received the bachelor's degree in engineering mechanics from China Jiliang University, in 2017. He is currently pursuing the master's degree in electrical engineering with Xi'an Jiaotong University. From 2017 to 2018, he worked as a Metrology Engineer with Hangzhou Enterprise. His current research interests include electrical cables and optical fiber communication.

JING YU was born in China, in 1973. She graduated in 1995. After graduation, she started to work at the Shanghai Electric Cable Research Institute. She has participated in the national "863" scientific and technological project research and development of optoelectronic composite cable detection technology for marine equipment, and is also one of the core research members of the National Key Research and Development Plan Project "Research and Demonstration of Key Technologies for Power Fiber to the Home." She has actively participated in the preparation of a large number of national and industry-related technical standards.

YONGHONG CHENG (Senior Member, IEEE) was born in Anhui, China, in 1965. He received the M.S. and Ph.D. degrees in electrical engineering from Xi'an Jiaotong University, Xi'an, China, in 1991 and 1999, respectively.

Since 2001, he has been a Professor at Xi'an Jiaotong University. His research interests include the property of dielectric materials, failure mechanism of insulating materials under extreme conditions, aging mechanism of insulation in power equipment, online detecting, and diagnosis technique on electrical insulation. He has been awarded several research prizes in China. He was awarded the Chang Jiang Scholar Professor in 2009. He is a member of General Test Special Committee, General Armament Department in China, and a member of Committee of ETSC of China Electro-Technical Society.